Colloid Polym Sci (2017) 295:1391–1403
DOI 10.1007/s00396-017-4083-z

INVITED ARTICLE

Conformational behavior of polymer chains of different architectures in strongly endothermic solvent mixtures: specific solvation effects

Lucie Suchá [1] · Zuzana Limpouchová [1] · Karel Procházka [1,2]

Received: 18 January 2017 / Revised: 21 March 2017 / Accepted: 25 March 2017 / Published online: 20 April 2017

Abstract Preferential solvation of polymer chains by the thermodynamically better component in mixed solvent is a general phenomenon which has been amply studied in systems of miscible solvent components. In strongly endothermic mixtures of partially miscible solvent components, it provokes transient contraction of polymer chains and can lead to cononsolvency, which consists in the fact that a mixture of two good solvents becomes a poor solvent. It has been studied for a few polymers and solvent mixtures, but so far, there is not a consensus concerning the principles of this behavior at the molecular level. We performed a series of coarse-grained dissipative particle dynamic simulations aimed at broadening the knowledge of preferential solvation in endothermic mixtures. The study shows that the cononsolvency can be partially explained by general thermodynamic arguments at coarse-grained the mean-field level, but the model ignoring specific interactions fails to describe all details correctly.

Keywords Cononsolvency · Preferential solvation · Dissipative particle dynamics · Linear polymer · Star polymer · Polymeric dendrimer

✉ Zuzana Limpouchová
zl@natur.cuni.cz

[1] Department of Physical and Macromolecular Chemistry, Faculty of Science, Charles University, Hlavova 2030, 128 40 Prague, Czech Republic

[2] Laboratory of Chemistry and Physics of Aerosols, Institute of Chemical Process Fundamentals of the CAS, v. v. i., Rozvojová 135/1, 165 02 Prague 6, Czech Republic

Introduction

Specific (or often called preferential) solvation of polymer chains is a general phenomenon which significantly affects the behavior of polymers dissolved in solvent mixtures. In most exothermic or enthalpically neutral mixed solvents, favorable interactions of the thermodynamically better solvent component with structural units of the chain lead to the increase of its content in polymer coil domain as compared with the composition of bulk solvent. It follows that preferential solvation usually facilitates polymer dissolution and promotes the expansion of dissolved chains. This phenomenon and its consequences have been amply studied by refractive index increment measurements under osmotic equilibrium of low-molar-mass components in combination with light scattering [1], and at present, it represents a fairly well-understood topic treated in polymer textbooks [2].

However, the preferential solvation of chains in mixed solvents containing components, mutual interaction of which is very unfavorable (strongly endothermic mixtures), has been studied only for a limited number of solvents in spite of the fact that it generates very interesting effects. If a polymer is dissolved in a fairly good solvent A and a small amount of a slightly better solvent B which interacts very favorably with the chain and unfavorably with the majority solvent component A is added, molecule B solvates preferentially the chain and simultaneously try to avoid contacts with the majority solvent component A. The conformational behavior of the polymer is strongly affected, because the chain solvated by firmly "bound" molecule B interacts with the majority solvent A via unfavorable A-B interactions. The attempt to minimize the number of unfavorable contacts in A-B results in chain collapse. Depending on the strength of interactions, it was proposed that chain collapse induced by preferential solvation can generate macroscopic phase separation, called

"cononsolvency." The above-outlined simplified explanation of experimentally observed cononsolvency has been later reexamined, criticized, and modified by a number of research groups. However, in spite of a number of studies devoted to this topic, so far there is no consensus concerning the reasons of this peculiar behavior [3–16].

The "cosolvency" and "cononsolvency" are intriguing phenomena which appear in solutions of certain solutes (usually polymers) in mixed solvents. While cosolvency, consisting in the fact that a mixture of several poor solvents is a better solvent for the same solute than any of pure solvent components, is a relatively common phenomenon, cononsolvency (the opposite case) is a fairly rare occurrence. The term cononsolvency was first used by Wolf and Willms in their study of the solution behavior of polystyrene in cyclohexane-dimethylformamide mixtures in 1978 [17]. Note that the mixing of dimethylformamide with hydrocarbons is strongly endothermic. For example, the maximum value of the heat of mixing of dimethylformamide with heptane is ΔH_{mix} = 0.63 kJ/mol for x_{Hept} = 0.56 and t = 25 °C [18], and the mixtures with cyclohexane are even more endothermic and only partially miscible.

The best-known and the most-studied example is the behavior of poly(*N*-isopropylacrylamide) (PNIPAM) in methanol-water mixtures at ambient and slightly elevated temperatures [3–14]. However, the behavior of this particular system is very complex and is strongly affected by the anomalous behavior of the solvent mixture. Methanol and water are well miscible, their mixing is strongly exothermic [19], but it has been known for a long time that the properties of methanol-water mixtures are very asymmetric at low methanol contents. The partial molar volume of methanol passes minimum at x_{Met} ca. 0.15 [20], and the thermodynamic functions of mixing are quite small as compared with those for ideal mixing. The structural origin of the non-ideal behavior has been many times analyzed and discussed in several review articles (see, e.g., [21]). Modern scattering techniques (X-ray and neutron scattering) indicate strongly inhomogeneous mixing in the whole concentration range [22, 23]. Advanced experimental techniques on the one hand and targeted computer simulations on the other hand [24, 25] significantly contributed to the broadening of our knowledge of the behavior of methanol-water mixtures, but they did not unambiguously solve the problem of anomalies at low methanol contents.

It is obvious that the conformational behavior and solubility of PNIPAM in methanol-water mixtures depend strongly on the number and on the strength of hydrogen bonds formed between individual components under different conditions. The Gibbs free energy balance is quite complex and comprises (i) the enthalpy of hydrogen bonds between polymer units and solvent, (ii) the enthalpy and entropy contributions reflecting the changes of the solvate shell "structure," and (iii) the conformational entropy of polymer chains. The slightly acidic (partially positively charged) hydrogen atoms from –OH groups can participate in hydrogen bond formation with water molecules, but the methyl group are strongly hydrophobic and their interaction with water molecules is unfavorable. The amphiphilic character of CH_3OH promotes hydrogen bonding between water molecules in the solvation layer of the methyl group (water oligomers bonded via hydrogen bonds are less polar than single molecules), and the exothermic effect is a result of increasing fraction of hydrogen bonds between H_2O molecules.

Behavior of PNIPAM was recently studied by Kremer et al. by a combination of a number of experimental methods (NMR, light scattering, etc.), atomistic molecular dynamic simulation, and mean-field theory [26–29]. These authors offered fairly convincing explanations of a number of experimentally observed effects on the basis of a fairly general approach. Some of their results were analyzed and criticized by Graziano et al. [30], but the papers by Kremer represent nice pieces of theoretical research aimed at generalized explanation of intriguing effects in polymer solutions.

However, PNIPAM is not the only example of practically important polymers, the solubility of which worsens in mixed solvents. There exist a number of other practically important neutral polymers, the solubility of which is negatively affected by preferential solvation. Poly(ethylene oxide) (PEO), poly(alkyl-oxazolines) (PAOX), poly(methacrylic acid) (PMAA), etc. are the polymers which dissolve both in polar organic solvents and in water and have been employer in a number of experimental studies. Note that PMAA is negligibly dissociated in aqueous mixtures rich in organic component and behaves as a non-polar (fairly hydrophobic) polymer. The most commonly used solvents in polymer research that are miscible with water are tetrahydrofuran (THF) and 1,4-dioxane (DOX). Their mixtures with water do not behave as ideal liquid mixtures. The dependence of heat effects accompanying their mixing with water is quite complex: Water-rich mixtures are exothermic, while DOX-rich or THF-rich mixtures are endothermic [31, 32]. The sign of heat effect changes approximately in one-to-one mixtures (it depends on temperature). It is obvious that $\Delta H_{mix} > 0$ in DOX-rich mixtures is a result of the "dilution" of water molecules in DOX and reflects the replacement of strong H bonds between water molecules by weaker H bonds between water hydrogen atoms and oxygen atoms in DOX molecules. The mixtures of DOX and THF with water and solvation of various organic molecules dissolved in these mixtures have been studied by different experimental methods [33–38] and also by computer simulation [39]. Their results indicated non-random mixing and important formation of clusters of molecules both types. In the region of water-rich mixtures, all experimental studies revealed the increase of "water structure"

(formation of hydrogen bonds between water molecules) and non-monotonous dependences of a number of properties on the content of organic component.

Systematic studies targeted at the stability of polymer solutions other than PNIPAM in aqueous mixtures with organic components are rare. In our experimental studies aimed at the preparation of self-assembled copolymer nanoparticles decorated by protective PMAA or PEO shells via the stepwise or continuous dialysis in DOX-water or THF-water mixtures, we observed peculiar behavior and decreased stability of copolymer solutions in solvents containing excess of organic component. Therefore, we elaborated and used the preparation protocol avoiding solvent mixtures with less than 20 vol% of H_2O [40–44].

The solution behavior of PMAA, PEO, or PAOX in DOX-rich mixtures mimics the behavior of strongly endothermic solvent mixtures in which the transient worsening of polymer solubility can be expected. The primary goal of this paper is to investigate if or to what extent the behavior of polymers in endothermic mixtures can be (in the first approximation) reproduced and elucidated by coarse-grained simulations based on a simple model The study should give clear answer if the coarse-grained approach (ignoring specific interaction effects) can reasonably emulate the intriguing phenomenon of cononsolvency or not. The cononsolvency is a very attractive topic, and it would be very beneficial to find a simple general explanation at the level of mean-field description. We would like to make clear that we do not address the behavior of polymers in exothermic mixtures, and therefore, we do not try to explain the behavior of PNIPAM in methanol-water mixtures.

However, the general aim of the study is relatively broad. We study the conformational behavior of model polymers of different architectures in a fairly wide range of parameters that describe interactions between individual components in endothermic solvent mixtures. A series of simulations should reveal the trends of the behavior and the extent of chain collapse in a broad range of compositions of solvent mixtures which are either fully or only partially miscible. We believe that dissipative particle dynamics (DPD), which has been successfully used for studying various complex polymer systems [45–47], is a suitable simulation technique for this purpose. Last but not least, we would like to exploit the knowledge on the behavior of polymers of different architectures in miscible endothermic mixtures in the research of separation processes and phase equilibria, particularly in the field of vapor-phase osmometry and combined size exclusion and interaction chromatography.

Dissipative particle dynamics

DPD is a coarse-grained molecular dynamic method with explicit solvent developed by Hoogerbrugge and Koelman [48] and further modified by Groot, Warren, Español, and others [48–51]. It employs three types of forces: (i) a soft conservative force, $\boldsymbol{F}^C$ which describes the interaction between the coarse-grained beads; (ii) a dissipative force, $\boldsymbol{F}^D$ which emulates friction; and (iii) a random force, $\boldsymbol{F}^R$ which reflects thermal agitation and intermolecular collisions.

$$\boldsymbol{F} = \boldsymbol{F}^C + \boldsymbol{F}^D + \boldsymbol{F}^R \tag{1}$$

$\boldsymbol{F}^C$ is given as the negative derivative of the particle coarse-grained potential, u^{CG}, i.e.,

$$\boldsymbol{F}^C = -\nabla_{\boldsymbol{r}} u^{CG} \tag{2}$$

The forces, $\boldsymbol{F}^D$and $\boldsymbol{F}^R$, which replace a number of degrees of freedom neglected by the coarse-graining approach, are given by

$$\boldsymbol{F}_{ij}^D = -\gamma_{ij}\ \omega^D(r_{ij})\ \left(\frac{\boldsymbol{r}_{ij}}{r_{ij}}\cdot\boldsymbol{v}_{ij}\right)\ \frac{\boldsymbol{r}_{ij}}{r_{ij}} \tag{3}$$

and

$$\boldsymbol{F}_{ij}^R = \sigma_{ij}\ \omega^R(r_{ij})\ \frac{\zeta_{ij}\ \boldsymbol{r}_{ij}}{\sqrt{\Delta t}\, r_{ij}} \tag{4}$$

where $\boldsymbol{r}_{ij} = \boldsymbol{r}_i - \boldsymbol{r}_j$ is the separation vector between particles i and j, $r_{ij} = |\boldsymbol{r}_{ij}|$, $\omega^D(r)$, and $\omega^R(r)$ are weight functions that vanish for $r \geq r_c$, r_c is the cutoff radius, γ_{ij} is the friction coefficient, σ_{ij} is the noise amplitude, $\boldsymbol{v}_{ij} = \boldsymbol{v}_i - \boldsymbol{v}_j$ is the relative velocity, $\xi_{ij} = \xi_{ji}$ is a Gaussian random number with zero mean and unit variance that is chosen independently for each pair of interacting particles, and Δt is the time step. The pairwise nature of dissipative and random forces guarantees that the momentum is conserved locally, which, in turn, ensures the correct hydrodynamic behavior.

The dissipative force and the random force have to be well balanced to provide correct distribution of particle velocities described by the Maxwell-Boltzmann distribution function at a given temperature, i.e., to secure a constant temperature of the system during the simulation run. Español and Warren [50] showed that the simulation technique samples the canonical ensemble when the forces obey the fluctuation-dissipation theorem if the following relationships hold:

$$\omega^D(r) = \left[\omega^R(r)\right]^2 \tag{5}$$

$$\sigma_{ij}^2 = 2\gamma_{ij}kT \tag{6}$$

$\omega^D(r)$ and $\omega^R(r)$ are typically chosen [49, 51] as

$$\omega^D(r) = \left[\omega^R(r)\right]^2 = \begin{cases} \left(1-\dfrac{r}{r_c}\right)^2 & (r_{ij} < r_c) \\ = 0 & (r \geq r_c) \end{cases} \tag{7}$$

Technically speaking, the application of the fluctuation-dissipation theorem plays the role of a thermostat; however, in a more profound physical context, it substitutes the effect of a number of fast and spatially restricted motions

(vibrations and rotations of parts of coarse-grained beads due to short-range interactions), that were sacrificed in favor of coarse graining and accelerating the calculations.

The evolution of the system, i.e., the motion of the DPD particles in time t, is governed by Newton's equations of motion

$$\frac{d\boldsymbol{r}_i}{dt} = \boldsymbol{v}_i$$
$$m_i \frac{d\boldsymbol{v}_i}{dt} = \boldsymbol{F}_i = \sum_{i \neq j} \left(\boldsymbol{F}_{ij}^C + \boldsymbol{F}_{ij}^D + \boldsymbol{F}_{ij}^R \right) \quad (8)$$

Similarly to other coarse-grained methods, the DPD approach focuses on the description of effective forces acting between larger parts of the system (coarse-grained beads). The pair interactions between beads i and j are "soft" and do not diverge at short distances r_{ij}, which means that the beads are also soft and can interpenetrate each other. The original DPD method developed for studies of systems without electrically charged components employs the soft spatially limited repulsion as the only non-bonding conservative force

$$u_{ij}^{sr} = \frac{a_{ij}}{2} r_c \left(1 - \frac{r_{ij}}{r_c}\right)^2 \quad (r_{ij} < r_c)$$
$$= 0 \quad (r_{ij} \geq r_c) \quad (9)$$

where a_{ij} is the maximum repulsion between particles i and j.

The fact that the soft conservative forces in the original DPD variant have been exclusively repulsive deserves two explanatory comments: First, the simulation method has to secure the condition that the particles constituting the fluid system are kept (by an external implicit force) in the simulation box at a predefined average density. This condition is achieved if the repulsive forces are calibrated on the basis of the dependence of solvent compressibility on density. Second, the attraction between some components of the system is treated as a weaker repulsion compared to the interaction among other components of the system. In this respect, the relative description of pair interactions is reminiscent of the Flory-Huggins (FH) treatment of interactions in the lattice theory of concentrated polymer solutions [52].

Although several different coarse-grained parameterization procedures were published [51, 53–56], in most studies published so far, one solvent bead represents three molecules of water [51, 53, 57]. If macromolecular systems are studied, polymer chains are usually modeled as strings of coarse-grained particles which are connected by elastic springs and form a flexible chain. The harmonic spring potential is used to describe the bond strength and elasticity:

$$u_{i,i+1}^{hs} = \frac{K}{2} \left(r_{i,i+1} - r_0\right)^2 \quad (10)$$

The potential of the elastic force represents the second type of conservative force. It is worth mentioning that polymer chains in DPD are the coarse-grained bead-spring chains, which is slightly confusing from the nomenclature point of view because this term is currently used for less coarse-grained chains, the beads of which interact via the Lennard-Jones potential [58]. The attraction among adjacent particles i and $i+1$ actually competes with the soft repulsive interaction. In Eq. (10), K is the spring constant and r_0 is the equilibrium distance. Groot and Warren have shown that values of $K/(kT)$ (k is the Boltzmann constant and T is the temperature) between 2 and 4, together with $r_0 = 0$, are convenient for modeling typical real polymers, since this choice prevents excessive bond stretching (weak springs).

Groot and Warren [49] mapped DPD results onto FH systems and established a link between the DPD parameters of soft repulsive forces a_{ij} and the FH interaction parameter χ_{ij}, which describes the interaction of FH segments.

$$\chi_{ij} = 2\alpha\rho r_c^3 \left(a_{ij} - a_{ii}\right) \frac{r_c}{kT} \quad (11)$$

where ρ is the total particle density and α is a proportionality constant dependent on ρ. Using the appropriate equation of state for the soft repulsive DPD fluid together with the value of compressibility for ambient water, and assuming $a_{ii} = a_{jj}$, they derived for polymer systems at $\rho r_c^3 = 3$ the following simple relation

$$\frac{a_{ij} r_c}{kT} = \frac{a_{ii} r_c}{kT} + 3.27\chi_{ij} \quad (12)$$

We would like to remind the reader that $a_{ij} = 25$ corresponds to $\chi = 0$, i.e., it emulates favorable interactions between the components, $a_{ij} = 26.64$ describes θ state ($\chi = ½$) and $a_{ij} = 40$ describes strongly unfavorable interactions corresponding to $\chi = 4.587$. Even though the choice of the level coarse graining is a priori a free in DPD, the fact that the parameters of interaction potentials have been recalculated from the Flory χ_{ij} parameter, which is based on interactions between the Kuhn segments, a posteriori sets the scale of coarse graining at the level of Kuhn segments because the parameters should describe forces acting between corresponding coarse-grained parts of the chain in both models. This fact is important because it enables a straightforward comparison of simulation results with predictions of standard theories of polymer solutions which are based on the same level of coarse graining.

Model

We mimic the behavior of dilute homopolymer solutions using (i) linear chain, (ii) polymer star, and (iii) the third-generation polymer dendrimer, all containing 226 beads connected by harmonic springs (except the star which is composed of six arms and contains 223 beads) (Scheme 1). The dendrimer contains three levels, and the functionality of branching points is 3.

Scheme 1 The architectures of studied polymers

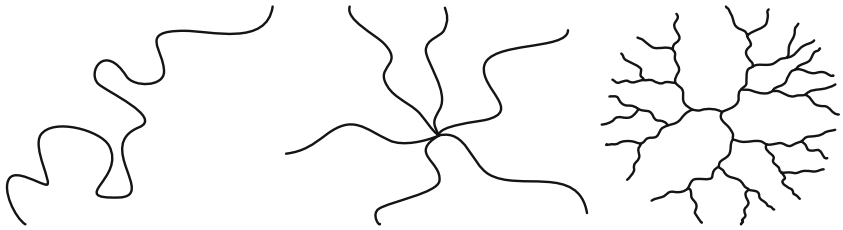

The length of linear parts between branching points is five beads. We place only one polymer species in the simulation box which contains a mixture of solvent particles A and B of different compositions. The size of the simulation box is 22, and the volume fraction of polymers in the system was $\varphi_P = 0.007$ in the overwhelming majority of simulations. In the DPD method, the following reduced units were used: r_c is the unit of length, the unit of mass is the mass of a DPD particle, and the unit of energy is kT; these terms are used throughout this work. All the DPD simulations were carried out at a total particle density of $\rho = 3$ in a cubic box of 22^3 with noise amplitude $\sigma_{ij} = 3$ and time step $\Delta t = 0.05$.

Using the reduced units, we set the repulsion parameter between like particles at $a_{ii} \equiv a_{jj} = 25$. We assume that the solvent A is thermodynamically good ($a_{PA} = 25$) and the solvent B is even slightly better ($a_{PB} = 20$), but the mutual A-B interaction is unfavorable (the mixing of A and B is strongly endothermic). Therefore, we vary the A-B interactions in a fairly broad range $a_{AB} = 32–40$. The above parameters correspond to the bead-bead χ interaction parameters, 2.141–4.587, respectively. For the harmonic spring potential, we used the spring constant $K = 4$ and equilibrium distance $r_0 = 0$.

In order to explain the choice of interaction parameters and help the reader to orient in the next paragraph, we would like to recall that $a_{ij} = 25$ (corresponding to $\chi = 0$) describes in DPD the interaction between favorably interacting particles, i.e., either interactions between identical particles ($a_{ij} = a_{ii}$) or cross interactions in athermal systems when $a_{ij} = (a_{ij} - (a_{ii} + a_{jj}) / 2) = 0$. The polymer solvent interaction $a_{ij} = 26.64$ (corresponding to $\chi = 1/2$) models the behavior of polymers in θ solvents, when somewhat stronger mutual interactions between polymer beads than those between polymer beads and solvent molecules fully compensate the effect of excluded volume and the self-avoiding chains behave like the interpenetrating chains. It is necessary to bear in mind (even if it is not very important in this study) that the chains in simulation studies are significantly shorter than the real ones, and therefore, the commonly used interaction parameters are usually higher than those obtained in experimental studies. The recalculation is based on the relation that sets the condition for phase separation in polymer blends, i.e., $N\chi = 10$ (i.e., $N_1\chi_1 = N_2\chi_2$), where N_i are the lengths of respective chains. The value $a_{ij} = 20$, which corresponds to $\chi = -1.53$, describes specific attractive interaction between polymer units and solvent molecules. In the studied systems, it reflects the formation of hydrogen bonds between oxygen atoms in PEO or in PAOX and hydrogens in H_2O. Solvent mixtures (DOX-H_2O or THF-H_2O) do not obey the behavior of regular solutions, but the values of interaction parameters between components of the solvent mixture can be easy elucidated using the concept of regular solutions. The estimate of the heat of mixing $\Delta H_{mix} = RTx_1x_2\chi_{12}$ for $x_{DOX} = 0.82$ yields strongly endothermic values 0.78, 1.12, and 1.68 kJ/mol for $a_{ij} = 32$, 35, and 40, i.e., for $\chi_{12} = 2.15$, 3.6, and 4.59, respectively. For comparison, the maximum endothermic value ΔH_{mix} in DOX-H_2O mixture is $\Delta H_{mix} = 0.483$ kJ/mol for $x_{DOX} = 0.82$ and $t = 25$ °C [31], which means that the first value $\chi_{12} = 2.15$ is acceptable and models the solvent mixture (e.g., DOX-H_2O or cyclohexane-dimethylformamide) reasonably well, but the two higher values model systems with very unfavorable interactions.

Simulations typically started from random configurations, and after an equilibration period of 2×10^6 time steps, we typically ran $(20 - 50) \times 10^6$ time steps for aggregated systems and 5×10^6 time steps otherwise. DPD trajectories were generated using the GNU program DL_MESO [59], followed by post-processing to evaluate the quantities of interest. All other details can be found in our earlier publications [60–63].

Results and discussion

As it was already explained in the previous "Model" section, we performed the computer study of the conformational behavior of polymers composed of $N_P = 226$ (223 in case of the star) beads differing in polymer architecture in dilute solutions in mixed solvents. We use the DPD method and simulate only one chain in the simulation box, which corresponds to polymer volume fraction $\varphi_P = 0.007$. Figure 1 depicts the size characteristics (radius of gyration (R_G)) as a function of composition of the solvent mixture (molar fraction of better solvent B, x_B). Figure 1a, b, c shows the dependences of the radius of gyration (R_G) for linear chains, polymer stars, and polymer dendrimers, in solvent mixtures differing in mutual interaction: (a) for interaction parameter $a_{AB} = 32$, (b) for $a_{AB} = 35$, and (c) for $a_{AB} = 40$. Basic qualitative shape of all curves is similar. In mixtures containing less solvent B beads than polymer P beads (i.e., for $x_B < 0.007$), radii of gyration of

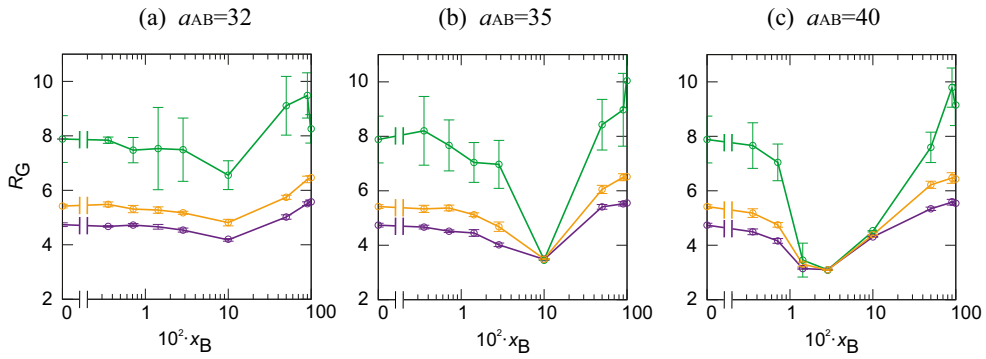

Fig. 1 Dependences of the radii of gyration (R_G) of studied polymer architectures on the composition of the solvent mixture (on molar fraction x_B). *Green curve* corresponds to linear chains, *yellow curve* to stars, and the *magenta curve* describes polymeric dendrimers. Interaction parameters used in DPD simulations are the following: a_{PA} = 25 (good solvent A), a_{PB} = 20 (good solvent B—slightly better than A); parameter a_{AB} describing unfavorable mutual interaction of solvent components varies in the range: a_{AB} = 32 (in **a**), a_{AB} = 35 (in **b**), and a_{AB} = 40 (in **c**). Standard deviations of simulated data are depicted by *error bars*. In case of stars and dendrimers, the fluctuations of sizes are small and *error bars* are smaller than the symbols depicting individual data points

all chain architectures decrease only little. In mixtures containing comparable or slightly higher amounts of B beads than P beads (x_B ca. 0.01–0.02), R_G starts to decrease significantly and in mixtures containing 2–10 vol% of B, a clearly pronounced minimum is reached, and later, the size starts to increase again because the overall solvent quality of the mixture improves. The depths of minima on individual curves and their positions depend on unfavorable A-B interaction (described by a_{AB}). For a_{AB} = 32, the minimum is very shallow.

In Fig. 1a, the contraction of polymer domains and decrease in R_G are negligible in spite of the fact that the value a_{AB} = 32 corresponds to the Flory-Huggins interaction parameter χ_{AB} = 2.141, i.e., to a non-negligibly endothermic mixture. For a_{AB} = 35 and 40, we see very pronounced transient decrease of R_G with increasing content of B. The changes of R_G are particularly obvious for linear chains, which form the most expanded coils in good solvents and simultaneously are the most deformable from all studied architectures. The radius of gyration in the good solvent A is $R_G \cong 9$ in reduced units and decreases almost 2.5 times to $R_{Gmin} \cong 3.5$ in a solvent with a_{AB} = 35, i.e., the volume decreases ca. 15 times which means that random polymer coil changes into very compact globule. When the incompatibility between solvent components further increases (a_{AB} = 40), the collapse occurs in solvent mixtures with a lower content of B, but the minimum size is approximately the same, which indicates that the chains form very compact conformations in both cases.

To prove the indirect conclusion on the compactness of chain conformations, we performed simulations of linear chains differing in length, N_P from 75 to 226: in solvent mixture with a_{AB} = 35 and (i) x_B = 0.1 (constant B/A number ratio), (ii) in mixtures with constant ratio of numbers of B/P beads in the simulation box of constant size (the same as that for N_P = 226 and x_B = 0.1), and (iii) in mixtures with constant ratios of B/P and B/A (i.e., in a series of simulation boxes the size of which is proportional to the number of B beads). (i) The log R_G vs. log N_P plot for constant volume fraction of B beads (curve 1 in Fig. 2) yields the scaling exponent ν ca. 0.23, which is lower than the value describing the scaling of compact spheres. This finding is interesting; however, it is easy understandable. It suggests that the composition of solvent mixture is not the only parameter that controls the conformational behavior but that the ratio of numbers of B/P beads also plays a role. The simulation confirms that both short and long chains are strongly collapsed. However, the B/P ratio in systems with shorter chains is higher than that for systems with longer chains, and therefore, some "excess" B beads, which are not engaged in solvation of shorter polymer chains, are solubilized inside the coil domain and slightly swell the coil. With increasing chain length, B/P ratio

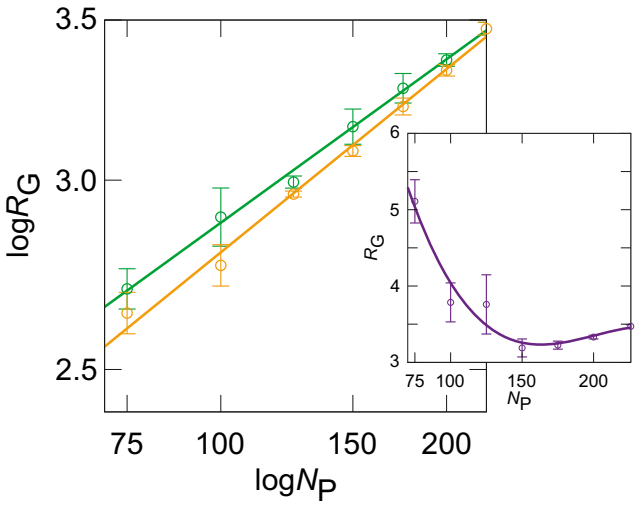

Fig. 2 Plots of radii of gyration of linear chains in mixtures of A and B components for a_{AB} = 35. Constant x_B (i.e., constant ratio of the numbers of B to A beads) (*green curve*); constant ratios of B/P and B/A beads (simulations in boxes of increasing size) (*orange curve*). Linear plot for constant B/P only (*inset*)

decreases and the "swelling" diminishes. This explains why the scaling exponent is very low.

(ii) The attempt to provide the log-log scaling plot in mixtures with constant ratio of numbers of B/P beads in the simulation box of constant size (the same as that for $N_P = 226$ and $x_B = 0.1$) failed completely. Therefore, we reproduced the linear plot R_G vs. N_P in the inset in Fig. 2. The shape of the curve is surprising. The dependence passes a pronounced minimum. However, the unexpected shape can be explained quite easy. It is obviously a result of entropy of small solvent molecules. In simulations for short chains, the volume fraction of B in the solvent mixture is quite low (ca. three times lower than that for the longest chain). An important fraction of B molecules, which should solvate the chain (because of enthalpy reasons), escapes into bulk solvent phase, and their considerable translational entropy hinders their engagement in the solvation of polymer chain. The fraction of B molecules in the solvation layer is low, and the chain collapse is only partial as compared with systems containing higher ratios of B/A. R_G for the shortest chains decreases with their length because the number of B beads in the simulation box increases and the solvation of the polymer by B improves until the optimum (almost complete) solvation by B beads is reached. Note that the optimum solvation is controlled both by enthalpy and entropy. In order to solvate the chain by B component, which is favorable from the enthalpy point of view, small mobile B beads actually condense on the chain and loose translational freedom (entropy). The interpretation of the observed conformational behavior is based on thermodynamic arguments which are reminiscent of those used for the explanation of hindered solvation of polymer chains and phase separation at LCST [64, 65].

(iii) The log-log plot for both B/P and B/A constant based on simulations in a series of simulation boxes with the length proportional to the third root of the number of B beads is again linear and yields slightly higher scaling exponent $\nu = 0.25$ as compared with the linear plot for constant B/A only. The scaling exponent is still lower than 0.33, which indicates that the conformations of longer chains are more compact than the conformations of shorter chains. The simulations thus confirm the fact that longer chains are more flexible than the shorter ones. The flexibility of chains is influenced by a number of factors (excluded volume of units, bond angles, rotational barriers, long range interactions, etc.) which reflect both enthalpy and entropy.

We added the curved dependence as the inset and discussed all three scaling plots purposely at length because the comparison demonstrates the complexity of the behavior, important role of entropy, and simultaneously, it clearly shows high danger of mechanistic misinterpretation of simulation data. To characterize the preferential solvation of polymer chains in a more quantitative manner, in Fig. 3a, b, we depict concentration profiles of P and B beads as functions of the distance from the center of gravity of the linear polymer chain and for the dendrimer in the mixture with $x_B = 0.028$ (four times higher number of B than P beads) and $a_{AB} = 40$, respectively. It is obvious that B beads (green curve) strongly accumulate in polymer domains and their concentration exceeds that of P beads (magenta curve) ca. twice—both for linear chain and for polymeric dendrimer. The concentrations of P beads in a good solvent A are shown by black curves for comparison. The concentrations of polymer beads in the expanded polymer domains in solvent A are very low in both cases (particularly in the case of linear chain), but one should keep in mind that the total number of polymer beads is given by the formula $N_P = 4\pi\int_0^{r_{max}} \rho(r) r^2 dr$.

At the first glance, it seems that simulations based on a general mean-field-like description of effective interactions without specific effects emulate general trends of the behavior of polymer in cononsolvent mixtures quite well. However, one has to be careful when analyzing and interpreting the simulation outcomes. The solvent components A and B which interact very unfavorably with each other are usually only

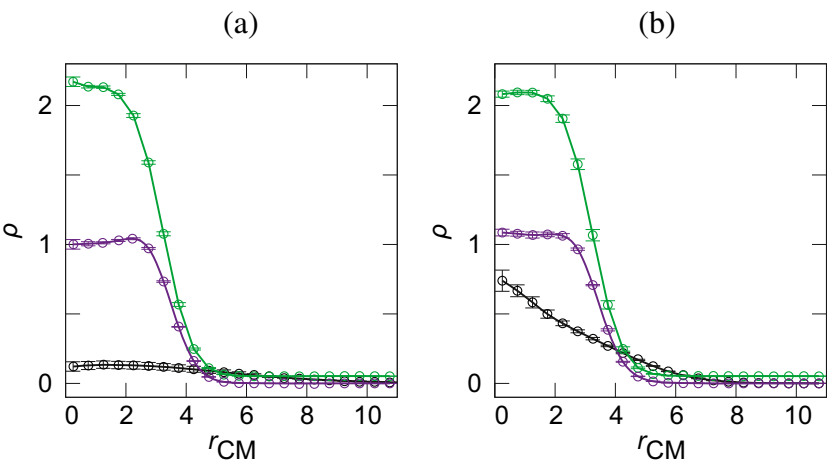

Fig. 3 Concentration profiles of beads in collapsed polymer structures (**a** linear chain and **b** polymeric dendrimer) in a solvent mixture with $x_B = 0.028$ (four times higher number of B than P beads) and $a_{AB} = 40$, respectively. *Green curves* correspond to B beads and *magenta curves* to polymer P beads. *Black curves* depict the concentration profiles of polymer P beads in expanded structures dissolved in pure solvent A

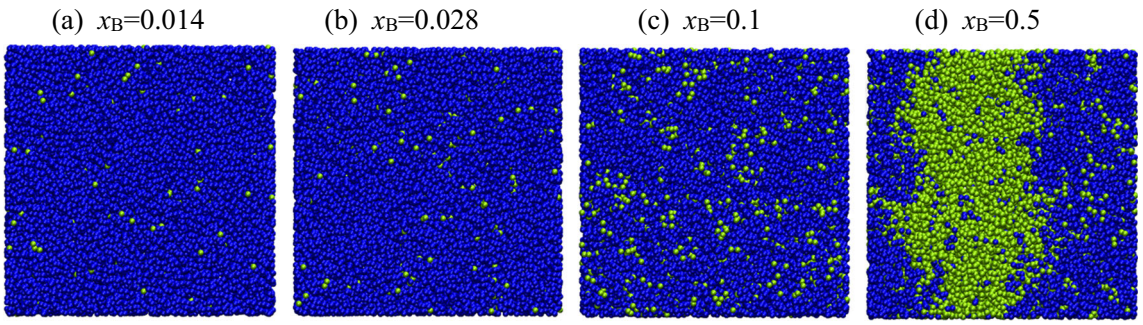

Fig. 4 Typical snapshots of the simulation box containing the mixtures of unfavorably interacting solvent components A and B (interaction coefficient a_{AB} = 35) for increasing content of solvent B. **a** x_B = 0.014. **b** x_B = 0.028. **c** x_B = 0.1. **d** x_B = 0.5. A beads are depicted by *blue color* and B beads by *green color*

partially miscible. When we study almost infinitely dilute polymer solutions, the number of B beads necessary for efficient solvation of the polymer chain in the mixture is low and the contraction of chain dimensions occurs at low contents of B, i.e., still in one-phase system. At higher polymer concentrations, the decrease of chain dimensions and the minima on R_G vs. x_B curves shift to higher x_B values, i.e., into the immiscibility region because the parameters that control the conformational behavior are both x_B and the ratio of the numbers of B beads to P beads. Therefore at higher polymer concentrations, the separation of the mixture into two liquid phases will occur and polymer chains will redistribute into coexisting phases. Because the component B is a better solvent for the polymer, the concentration of polymer chains in the B-rich phase will be higher and the chains will be more expanded as compared with the A-rich phase.

To be honest, our simulations for one chain in the simulation box in mixtures with moderately high contents of B can be also affected by phase separation. Therefore, we simulated several liquid mixtures (without polymer chain) with increasing contents of B for interaction constants a_{AB} = 35 and 40. Results for a_{AB} = 35 and 40 are depicted in the form of typical snapshots of the simulation box in Figs. 4 and 5, respectively. It is obvious that both 1:1 mixtures are immiscible, but the interface between coexisting phases is quite diffuse for the system with a_{AB} = 35; it suggests that the system is not too far from the separation condition. The most important result concerns the mixtures with x_B = 0.1, which belong to the region of the transient contraction of radii of gyration: While the solvent mixture with a_{AB} = 35 is still well miscible at x_B = 0.1, the increase in incompatibility of A and B components to a_{AB} = 40 leads to phase separation at x_B = 0.1.

Now, we can reanalyze simulation results on the transient collapse of polymer conformations in dilute solutions and interpret the conformational behavior correctly in detail with the help of the knowledge on the miscibility/immiscibility of liquid mixtures with increasing content of component B. In Fig. 6 (a–c), we present typical snapshots depicting the conformations of linear chains in mixtures, the behavior of which was shown in Fig. 4a–c, i.e., in mixtures of components with mutual interaction parameter a_{AB} = 35. In Fig. 6 (a–c), only the polymer P beads (magenta color) and minority solvent B beads are shown (green color), and in Fig. 6 (a′–c′), the conformations of polymer chains (without any solvent beads) are depicted to provide a comprehensive picture of the conformation behavior. It is obvious that all three mixtures are miscible, even though the intermixing of A and B does not seem to be fully random. Density profiles (not shown for this particular case—very similar to those shown in Fig. 3) indicate that component B concentrates in the polymer domain, but the

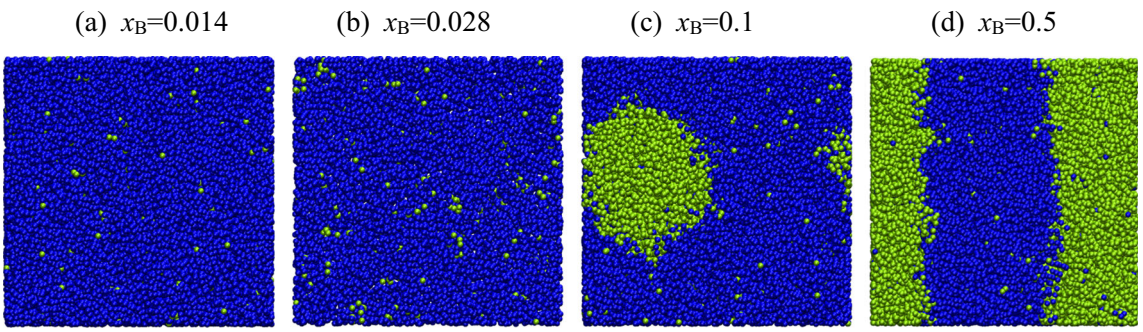

Fig. 5 Typical snapshots of the simulation box containing the mixtures of unfavorably interacting solvent components A and B (interaction coefficient a_{AB} = 40) for increasing content of solvent B. **a** x_B = 0.014. **b** x_B = 0.028. **c** x_B = 0.1. **d** x_B = 0.5. A beads are depicted by *blue color* and B beads by *green color*

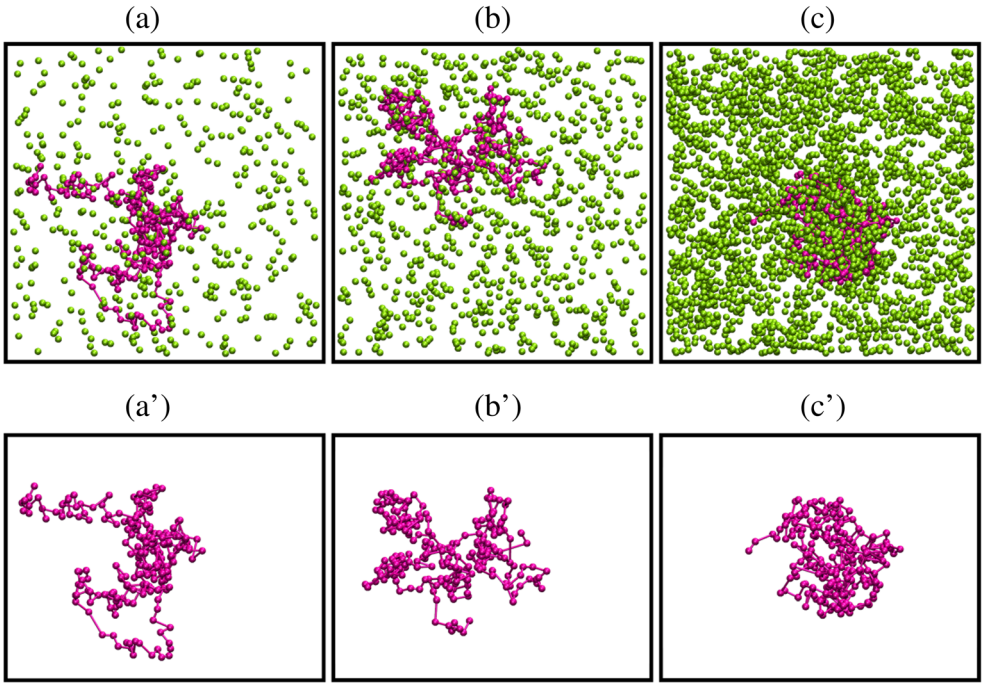

Fig. 6 Typical simulation snapshots depicting the conformations of linear chains composed of 226 beads in liquid mixtures of solvent components A and B (interaction coefficient $a_{AB} = 35$) for increasing content of component B: $x_B = 0.014$ (*a*), $x_B = 0.028$ (*b*), and $x_B = 0.1$ (*c*); B beads are depicted by *green color* and polymer P beads by *magenta color*. Bottom row (*a′–c′*) shows the structure of individual polymer structures without any polymer beads

presence of polymer in the mixture with $x_B = 0.1$ does not induce the liquid-liquid phase separation, i.e., the phase separation at a lower x_B value in comparison with the composition of pure solvent mixture that separates at a given temperature. It is clearly seen that the size of polymer domain decreases and its compactness increases with increasing content of B.

In Fig. 7, we present analogous data for polymeric dendrimers. All qualitative features of the conformational behavior are similar as in the previous case. The dendrimer structure shrinks with increasing x_B. While the linear chains contract continuously with increasing content of B in three depicted systems, the size and compactness of dendrimer structures change fast at low B contents, but it remains almost the same in the last two frames. The differences between dendrimers and linear chains reflect their different chain architectures. The architecture of the dendrimer, which is reminiscent of the unimolecular micelle, promotes the solubilization of species favorably interacting with P and unfavorably with

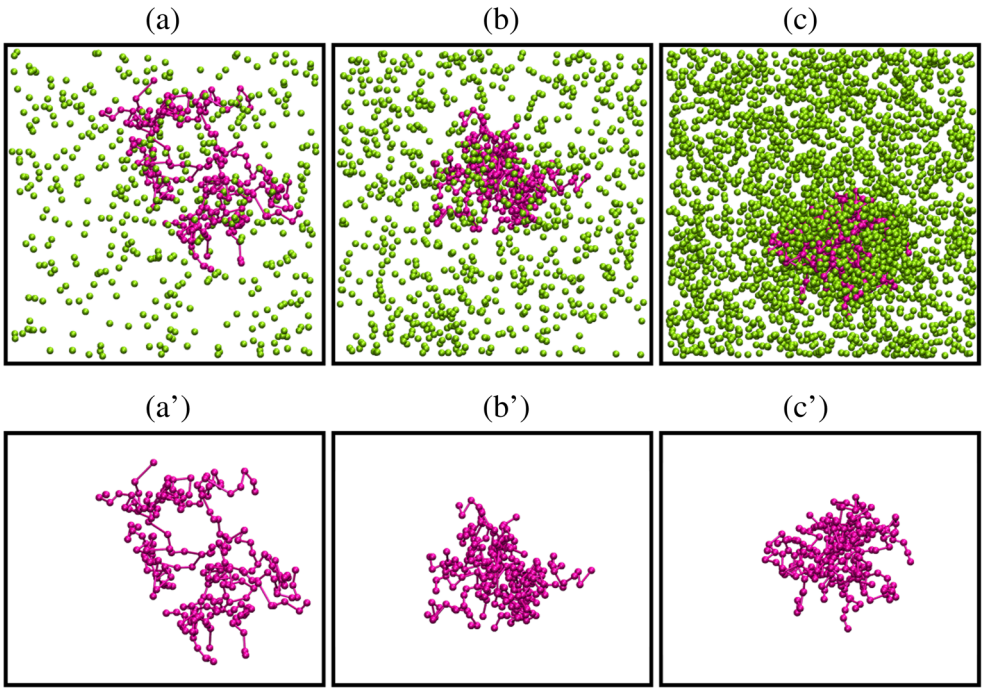

Fig. 7 Typical simulation snapshots depicting the conformations of polymeric dendrimers in liquid mixtures of solvent components A and B (interaction coefficient $a_{AB} = 35$) for increasing content of component B: $x_B = 0.014$ (*a*), $x_B = 0.028$ (*b*), and $x_B = 0.1$ (*c*); B beads are depicted by *green color* and polymer P beads by *magenta color*. Bottom row (*a′–c′*) shows the structure of individual dendrimer structures without any B beads

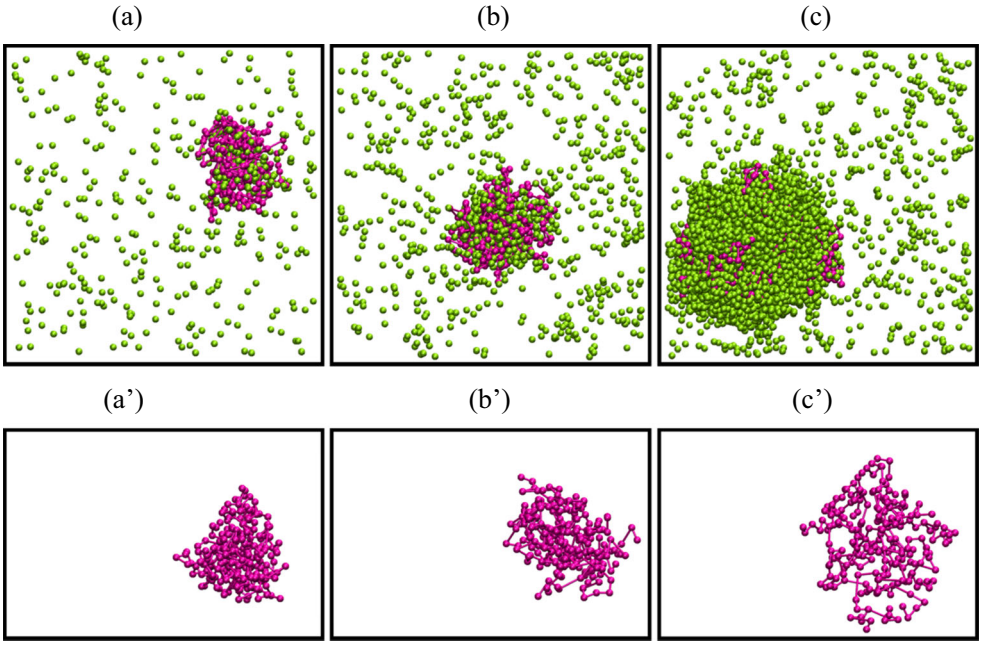

Fig. 8 Snapshots depicting the conformations of linear polymer chains in strongly incompatible solvent mixtures (interaction coefficient $a_{AB} = 40$) for increasing content of component B: $x_B = 0.014$ (*a*), $x_B = 0.028$ (*b*), and $x_B = 0.1$ (*c*); B beads are depicted by *green color* and polymer P beads by *magenta color*. The bottom row (*a′–c′*) shows the structure of individual polymer coils without any B beads

A into the dendrimer domain. The pronounced changes of dendrimer dimensions depicted in Fig. 7 at low contents of B indicate that appreciable uptake of B due to its preferential sorption (solubilization of component B into dendrimer domain) starts at lover B contents, but it slows down in mixtures with higher content of B simply because the collapsed dendrimer structure has been already strongly preferentially solvated and its compactness hinders further increase of the B content in the dendrimer domain.

The last two figures, Figs. 8 and 9, show typical snapshots of polymer conformations in mixtures with the most incompatible components A and B ($a_{AB} = 40$). It is obvious that in systems with low x_B, the polymeric structures are collapsed, but in the mixture with $x_B = 0.1$ (the frame c), both the linear chain and the polymeric dendrimer dissolve in the coexisting B-rich phase (we recall that the phases separate at a given composition in the absence of the polymer), and the chain conformation expands.

One should not forget that in systems containing high numbers of polymer chains, the partitioning of chains between two liquid phases would occur. On the basis of performed simulations, we assume that the intricate entropy-to-enthalpy

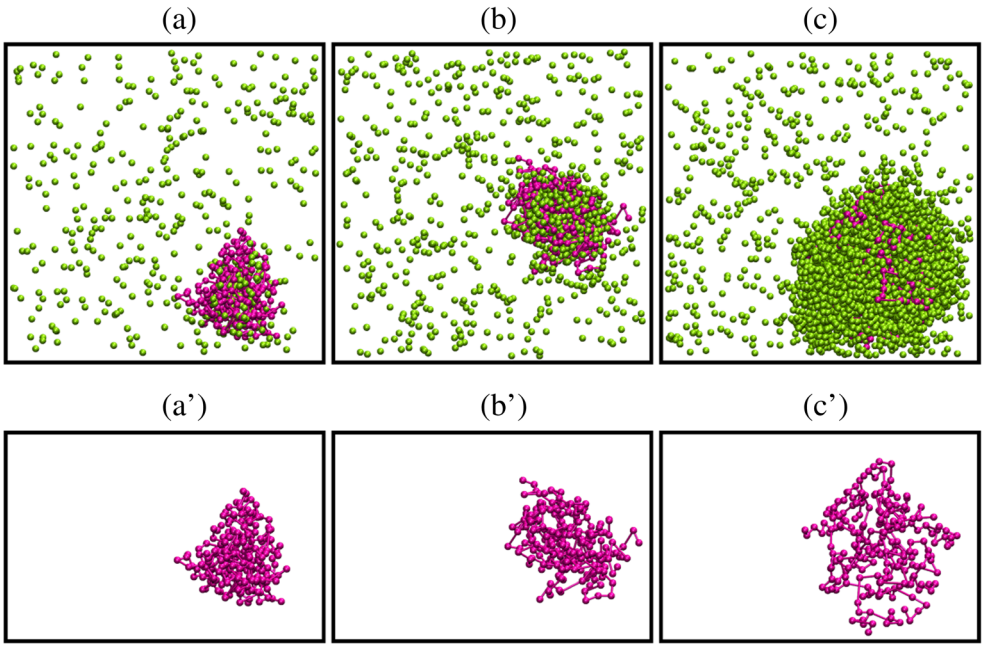

Fig. 9 Snapshots depicting the conformations of linear polymer chains in strongly incompatible solvent mixtures (interaction coefficient $a_{AB} = 40$) for increasing content of component B: $x_B = 0.014$ (*a*), $x_B = 0.028$ (*b*), and $x_B = 0.1$ (*c*); B beads are depicted by *green color* and polymer P beads by *magenta color*. The bottom row (*a′–c′*) shows the structure of individual dendrimer without any B beads

interplay would affect the partitioning equilibrium, i.e., the difference in thermodynamic quality of solvents A and B (based on enthalpic interactions only) does not seem to be the only characteristics controlling the partitioning of polymer chains of different architectures. The studies are in progress, and the results will be reported in our next publication as soon as possible.

Conclusions

Results of the study can be briefly summarized as follows: The coarse-grained DPD simulations reproduce correctly the conformational behavior of isolated polymer chains of different architectures in endothermic mixtures of good solvents. They emulate significant transient contraction of chains in mixtures containing relatively low contents of the better solvent which is incompatible with the majority solvent component.

However, the study simultaneously shows that the simplified mean-field-like approach fails to reproduce correctly the cononsolvency at finite polymer concentrations (even at low concentrations in the range 0.1 to 1.0 wt%) in systems, in which specific interactions play important role. The attempt to emulate sufficient collapse of chains, which would lead to appreciable worsening of polymer solubility in dilute and semidilute polymer solutions, by implicit inclusion of specific interaction effects into soft repulsion potentials requires to use very high repulsion parameters between solvent components. The amount of the better solvent necessary to induce the chain collapse is proportional to polymer concentration. Therefore in solutions containing finite polymer concentration, the cononsolvency would occur in the range of immiscible solvent compositions.

We would like to remind readers that the simple approach used in this study is conceptually reminiscent of the "effective solvent strength method" which has been proposed for simplified DPD simulations of polyelectrolytes [66]. In these simulations, the electrostatic interactions, which are important and modify the behavior considerably, are ignored at all and effective parameters of non-electrostatic interactions are used, the values of which depend on the fact if the monomer unit is charged or not. Similarly to the "solvent strength method," our DPD simulations with artificially increased repulsion parameters emulate the properties of chains in systems with appreciable specific interactions quite well, but some other characteristics of the systems are not consistent with experimental data (heats of mixing of solvent components, phase behavior, etc.). The study shows that a simple mean-field-like DPD treatment of systems with specific interactions does not guarantee correct simulation results.

However, a good news is that the performed simulations reproduce quite well the behavior of polymers in partially miscible endothermic mixtures, and hence, they can explain the cononsolvency of polystyrene in cyclohexane-dimethylformamide mixtures reported by Wolf and Willms [17].

The study indicates that the fairly compact polymer dendrimers have higher ability to solubilize traces of the minority solvent component (a slightly better solvent than the majority component) than the less branched polymer architectures. Even though the solubilization capacity of polymeric dendrimers is limited, properly designed dendrimer-based systems can serve as efficient scavengers of undesirable pollutants from liquid systems. An important indirect result of the study is the following:

Last, but not least, the results of simulations clearly show that the conformational behavior of polymers in mixed solvents is a result of intricate enthalpy-to-entropy interplay and that a superficial mechanistic interpretation of simulation data can lead to erroneous conclusions.

Acknowledgements This study was supported by the Czech Science Foundation (Grant No. P106-15-19542S) and by Grant Agency of the Charles University (Grant 422 216). Computational resources were provided by the CESNET LM2015042 and the CERIT Scientific Cloud LM2015085, provided under the program "Projects of Large Research, Development, and Innovations Infrastructures."

Compliance with ethical standards

Conflict of interest The authors declare that they have no conflict of interest.

References

1. Tuzar Z, Kratochvil P (1977) Extremely high refractive-index increments in polymer-mixed solvent systems. Macromolecules 10(5):1108–1110. doi:10.1021/ma60059a041
2. Kratochvíl P (1987) Light scattering from polymer solutions in mixed solvents. In: Kratochvíl P (ed) Classical light scattering from polymer solutions. Elsevier, Amsterdam-Oxford-New York-Tokyo
3. Chee CK, Hunt BJ, Rimmer S, Soutar I, Swanson L (2011) Time-resolved fluorescence anisotropy studies of the cononsolvency of poly(N-isopropyl acrylamide) in mixtures of methanol and water. Soft Matter 7(3):1176–1184. doi:10.1039/c0sm00836b
4. Tanaka F, Koga T, Kojima H, Winnik FA (2009) Temperature- and tension-induced coil-globule transition of poly(*N*-isopropylacrylamide) chains in water and mixed solvent of water/methanol. Macromolecules 42(4):1321–1330. doi:10.1021/ma801982e
5. Lin SY, Chen KS, Liang RC (1999) Thermal micro ATR/FT-IR spectroscopic system for quantitative study of the molecular structure of poly(N-isopropylacrylamide) in water. Polymer 40(10):2619–2624. doi:10.1016/s0032-3861(98)00512-6
6. Lin SY, Chen KS, Run-Chu L (1999) Drying methods affecting the particle sizes, phase transition, deswelling/reswelling processes and morphology of poly(N-isopropylacrylamide) microgel beads. Polymer 40(23):6307–6312. doi:10.1016/s0032-3861(98)00872-6

7. Chee CK, Rimmer S, Soutar I, Swanson L (1997) Time-resolved fluorescence anisotropy studies of the temperature-induced intramolecular conformational transition of poly(N-isopropylacrylamide) in dilute aqueous solution. Polymer 38(2): 483–486. doi:10.1016/s0032-3861(96)00636-2
8. Wu C, Zhou SQ (1995) Thermodynamically stable globule state of a single poly(n-isopropylacrylamide) chain in water. Macromolecules 28(15):5388–5390. doi:10.1021/ma00119a036
9. Otake K, Inomata H, Konno M, Saito S (1990) Thermal-analysis of the volume phase-transition with n-isopropylacrylamide gels. Macromolecules 23(1):283–289. doi:10.1021/ma00203a049
10. Kubota K, Fujishige S, Ando I (1990) Single-chain transition of poly(n-isopropylacrylamide) in water. J Phys Chem 94(12):5154–5158. doi:10.1021/j100375a070
11. Winnik FM (1990) Phase-transition of aqueous poly-(n-isopropylacrylamide) solutions—a study by nonradiative energy-transfer. Polymer 31(11):2125–2134. doi:10.1016/0032-3861(90)90085-d
12. Winnik FM, Ringsdorf H, Venzmer J (1990) Methanol water as a co-nonsolvent system for poly(n-isopropylacrylamide). Macromolecules 23(8):2415–2416. doi:10.1021/ma00210a048
13. Inomata H, Goto S, Saito S (1990) Phase-transition of n-substituted acrylamide gels. Macromolecules 23(22):4887–4888. doi:10.1021/ma00224a023
14. Yamamoto I, Iwasaki K, Hirotsu S (1989) Light-scattering study of condensation of poly(n-isopropylacrylamide) chain. J Phys Soc Jpn 58(1):210–215. doi:10.1143/jpsj.58.210
15. Prange MM, Hooper HH, Prausnitz JM (1989) Thermodynamics of aqueous systems containing hydrophilic polymers or gels. AICHE J 35(5):803–813. doi:10.1002/aic.690350511
16. Cowie JMG, Mohsin MA, McEwen IJ (1987) Alcohol water cosolvent systems for poly(methyl methacrylate). Polymer 28(9): 1569–1572. doi:10.1016/0032-3861(87)90360-0
17. Wolf BA, Willms MM (1978) Measured and calculated solubility of polymers in mixed solvents: co-nonsolvency. Die Makromolekulare Chemie 179(9):2265–2277. doi:10.1002/macp.1978.021790914
18. Quitzsch K, Strittma D, Geiseler G (1969) Thermodynamics of binary liquid mixtures with homologous formamides. 8. Binary systems normal-heptane (1)-dimethylformamide(2) and normal-heptane (1)-diethylformamide(2). Zeitschrift Fur Physikalische Chemie-Leipzig 240(1–2):107
19. Bertrand GL, Millero FJ, Wu CH, Hepler LG (1966) Thermochemical investigations of water-ethanol and water-methanol solvent systems. I. Heats of mixing heats of solution and heats of ionization of water. J Phys Chem 70(3):699–705. doi:10.1021/j100875a015
20. Aliev MM, Magee JW, Abdulagatov IM (2003) PVTx and isochoric heat capacity measurements for aqueous methanol solutions. Int J Thermophys 24(6):1551–1579. doi:10.1023/B:IJOT.0000004093.20692.dc
21. Franks F, Desnoyers JE (1985) Alcohol-water mixtures revisited. In: Felix F (ed) Water Science Reviews, vol 1. Cambridge University Press, UK, Cambridge
22. Dixit S, Crain J, Poon WCK, Finney JL, Soper AK (2002) Molecular segregation observed in a concentrated alcohol-water solution. Nature 416(6883):829–832. doi:10.1038/416829a
23. Dougan L, Bates SP, Hargreaves R, Fox JP, Crain J, Finney JL, Reat V, Soper AK (2004) Methanol-water solutions: a bi-percolating liquid mixture. J Chem Phys 121(13):6456–6462. doi:10.1063/1.1789951
24. Moucka F, Nezbeda I (2011) Water-methanol mixtures with non-Lorentz-Berthelot combining rules: a feasibility study. J Mol Liq 159(1):47–51. doi:10.1016/j.molliq.2010.05.005
25. Gonzalez-Salgado D, Nezbeda I (2006) Excess properties of aqueous mixtures of methanol: simulation versus experiment. Fluid Phase Equilib 240(2):161–166. doi:10.1016/j.fluid.2005.12.007
26. Mukherji D, Wagner M, Watson MD, Winzen S, de Oliveira TE, Marques CM, Kremer K (2016) Relating side chain organization of PNIPAm with its conformation in aqueous methanol. Soft Matter 12(38):7995–8003. doi:10.1039/C6SM01789D
27. de Oliveira TE, Netz PA, Mukherji D, Kremer K (2015) Why does high pressure destroy co-non-solvency of PNIPAm in aqueous methanol? Soft Matter 11(44):8599–8604. doi:10.1039/C5SM01772F
28. Mukherji D, Marques CM, Stuehn T, Kremer K (2015) Co-non-solvency: mean-field polymer theory does not describe polymer collapse transition in a mixture of two competing good solvents. Journal of Chemical Physics 142 (11). doi:10.1063/1.4914870
29. Mukherji D, Kremer K (2013) Coil-globule-coil transition of PNIPAm in aqueous methanol: coupling all-atom simulations to semi-grand canonical coarse-grained reservoir. Macromolecules 46(22):9158–9163. doi:10.1021/ma401877c
30. Pica A, Graziano G (2016) An alternative explanation of the cononsolvency of poly(N-isopropylacrylamide) in water-methanol solutions. Phys Chem Chem Phys 18(36):25601–25608. doi:10.1039/c6cp04753j
31. Goates JR, Sullivan RJ (1958) Thermodynamic properties of the system water-p-dioxane. J Phys Chem 62(2):188–190
32. Malcolm GN, Rowlinson JS (1957) The thermodynamic properties of aqueous solutions of polyethylene glycol, polypropylene glycol and dioxane. Trans Faraday Soc 53(7):921–931. doi:10.1039/tf9575300921
33. Takamuku T, Yamaguchi A, Tabata M, Nishi N, Yoshida K, Wakita H, Yamaguchi T (1999) Structure and dynamics of 1,4-dioxane-water binary solutions studied by X-ray diffraction, mass spectrometry, and NMR relaxation. J Mol Liq 83(1–3):163–177. doi:10.1016/s0167-7322(99)00083-5
34. Lee Y, Jonas J (1973) Pressure and concentration effects on molecular-reorientation in water-dioxane mixtures. J Chem Phys 59(9):4845–4854. doi:10.1063/1.1680697
35. Choppin GR, Violante MR (1972) Near-infrared studies of structure of water. 3. Mixed solvent systems. J Chem Phys 56(12):5890–589+. doi:10.1063/1.1677133
36. Hindman JC, Svirmick A, Wood M (1968) Deuteron spin-lattice relaxation of D2O in organic solvents. J Phys Chem 72(12):4188–418+. doi:10.1021/j100858a042
37. Garg SK, Smyth CP (1965) Microwave absorption and molecular structure in liquids. 66. Dielectric relaxation of water-dioxane system and structure of water. J Chem Phys 43(9):2959–295&. doi:10.1063/1.1697257
38. Fratiello A, Douglass DC (1963) NMR shift and diffusion study of Dioxane-H2O and pyridine-H2O mixtures. J Mol Spectrosc 11(6): 465–46&. doi:10.1016/0022-2852(63)90047-x
39. Sedov IA, Magsumov TI (2015) Thermodynamic functions of solvation of hydrocarbons, noble gases, and hard spheres in tetrahydrofuran-water mixtures. J Phys Chem B 119(28):8773–8780. doi:10.1021/acs.jpcb.5b04886
40. Humpolickova J, Stepanek M, Prochazka K, Hof M (2005) Solvent relaxation study of pH-dependent hydration of poly(oxyethylene) shells in polystyrene-block-poly(2-vinylpyridine)-block-poly(oxyethylene) micelles in aqueous solutions. J Phys Chem A 109(48):10803–10812. doi:10.1021/jp053348v
41. Matejicek P, Humpolickova J, Prochazka K, Tuzar Z, Spirkova M, Hof M, Webber SE (2003) Hybrid block copolymer micelles with partly hydrophobically modified polyelectrolyte shells in polar and aqueous media: experimental study using fluorescence correlation spectroscopy, time-resolved fluorescence, light scattering, and atomic force microscopy. J Phys Chem B 107(32):8232–8240. doi:10.1021/jp022221s

42. Matejicek P, Uhlik F, Limpouchova Z, Prochazka K, Tuzar Z, Webber S (2002) Experimental study of hydrophobically modified amphiphilic block copolymer micelles using light scattering and nonradiative excitation energy transfer. Macromolecules 35(25): 9487–9496. doi:10.1021/ma012074g
43. Podhajecka K, Stepanek M, Prochazka K, Brown W (2001) Hybrid polymeric micelles with hydrophobic cores and mixed polyelectrolyte/nonelectrolyte shells in aqueous media. 2. Studies of the shell behavior. Langmuir 17(14):4245–4250. doi:10.1021/la010247p
44. Stepanek M, Podhajecka K, Prochazka K, Teng Y, Webber SE (1999) Fluorometric and ultraviolet-visible absorption study of poly(methacrylic acid) shells of high-molar-mass block copolymer micelles. Langmuir 15(12):4185–4193. doi:10.1021/la981129d
45. Li Z, Dormidontova EE (2010) Kinetics of diblock copolymer micellization by dissipative particle dynamics. Macromolecules 43(7): 3521–3531. doi:10.1021/ma902860j
46. Posel Z, Posocco P, Fermeglia M, Lisal M, Pricl S (2013) Modeling hierarchically structured nanoparticle/diblock copolymer systems. Soft Matter 9(10):2936–2946. doi:10.1039/c2sm27360h
47. Sirk TW, Slizoberg YR, Brennan JK, Lisal M, Andzelm JW (2012) An enhanced entangled polymer model for dissipative particle dynamics. Journal of Chemical Physics 136 (13). doi:10.1063/1.3698476
48. Hoogerbrugge PJ, Koelman JMVA (1992) Simulating microscopic hydrodynamic phenomena with dissipative particle dynamics. Europhys Lett 19(3):155–160. doi:10.1209/0295-5075/19/3/001
49. Groot RD, Warren PB (1997) Dissipative particle dynamics: bridging the gap between atomistic and mesoscopic simulation. J Chem Phys 107(11):4423–4435. doi:10.1063/1.474784
50. Espanol P, Warren P (1995) Statistical-mechanics of dissipative particle dynamics. Europhys Lett 30(4):191–196. doi:10.1209/0295-5075/30/4/001
51. Groot RD, Rabone KL (2001) Mesoscopic simulation of cell membrane damage, morphology change and rupture by nonionic surfactants. Biophys J 81(2):725–736
52. Rubinstein M, Colby RH (2003) Polymer physics, chapter 4: thermodynamics of mixing. Oxford University, New York, pp. 137–170
53. Patterson K, Lisal M, Colina CM (2011) Adsorption behavior of model proteins on surfaces. Fluid Phase Equilib 302(1–2):48–54. doi:10.1016/j.fluid.2010.08.009
54. Fuchslin RM, Fellermann H, Eriksson A, Ziock H-J (2009) Coarse graining and scaling in dissipative particle dynamics. Journal of Chemical Physics 130 (21). doi:10.1063/1.3143976
55. Kacar G, Atilgan C, Ozen AS (2010) Mapping and reverse-mapping of the morphologies for a molecular understanding of the self-assembly of fluorinated block copolymers. J Phys Chem C 114(1):370–382. doi:10.1021/jp908324d
56. Kacar G, Peters EAJF, de With G (2013) A generalized method for parameterization of dissipative particle dynamics for variable bead volumes. Epl 102 (4). doi:10.1209/0295-5075/102/40009
57. Groot RD (2004) Applications of dissipative particle dynamics. In: Novel Methods in Soft Matter Simulations. Springer, pp 5–38
58. Frenkel D, Smit B (2001) Understanding molecular simulation: from algorithms to applications, vol 1. Academic press,
59. Seaton MA, Anderson RL, Metz S, Smith W (2013) DL_MESO: highly scalable mesoscale simulations. Mol Simul 39(10):796–821. doi:10.1080/08927022.2013.772297
60. Sindelka K, Limpouchova Z, Lisal M, Prochazka K (2014) Dissipative particle dynamics study of electrostatic self-assembly in aqueous mixtures of copolymers containing one neutral water-soluble block and one either positively or negatively charged polyelectrolyte block (vol 47, pg 6121, 2012). Macromolecules 47(20): 7252–7252. doi:10.1021/ma501978w
61. Posel Z, Limpouchova Z, Sindelka K, Lisal M, Prochazka K (2014) Dissipative particle dynamics study of the pH-dependent behavior of poly(2-vinylpyridine)-block-poly(ethylene oxide) Diblock copolymer in aqueous buffers. Macromolecules 47(7):2503–2514. doi:10.1021/ma402293c
62. Sindelka K, Limpouchova Z, Lisal M, Prochazka K (2016) The electrostatic co-assembly in non-stoichiometric aqueous mixtures of copolymers composed of one neutral water-soluble and one polyelectrolyte (either positively or negatively charged) block: a dissipative particle dynamics study. Phys Chem Chem Phys 18(24):16137–16151. doi:10.1039/c6cp01047d
63. Lisal M, Limpouchova Z, Prochazka K (2016) The self-assembly of copolymers with one hydrophobic and one polyelectrolyte block in aqueous media. Dissipative particle dynamics study. Phys Chem Chem Phys. doi:10.1039/C6CP00341A
64. Procházka K (2016) Conformational and dynamic behavior of polymer and polyelectrolyte chains in dilute solutions. In: Fluorescence Studies of Polymer Containing Systems. Springer, pp 1–26
65. Procházka K (2016) Fluorescence studies of polymer containing systems. Springer, Berlin
66. Li NK, Fuss WH, Yingling YG (2015) An implicit solvent ionic strength (ISIS) method to model polyelectrolyte systems with dissipative particle dynamics. Macromolecular Theory and Simulations 24(1):7–12. doi:10.1002/mats.201400043

Zuzana Limpouchová obtained her PhD degree in physical chemistry from the Faculty of Science, Charles University in Prague in 1991. After graduation, she joined the Department of Physical and Macromolecular Chemistry as assistant professor. She was promoted to associate professor in 2005. She specializes in computational studies of the conformational behavior and self-assembly of block copolymers and polyelectrolytes in aqueous media by Monte Carlo methods and by dissipative particle dynamics.